Journal of Ceramic Processing Research. Vol. 26, No. 4, pp. 559~566 (2025)
(Received 4 April 2025, Received in revised form 17 June 2025, Accepted 18 June 2025)
https://doi.org/10.36410/jcpr.2025.26.4.559

J O U R N A L O F
Ceramic Processing Research

Effects of blending bagasse with an aluminosilicate-based additive on bagasse ash properties

Ji Yeon Park[a,b], Byoung-In Sang[b], Kwonho Jeon[c], Sangmin Choi[c], Byoungdae Min[c] and Jin Hyung Lee[a,*]
[a]*Korea Institute of Ceramic Engineering and Technology, Cheongju 28160, Republic of Korea*
[b]*Department of Chemical Engineering, Hanyang University, Seoul 04763, Republic of Korea*
[c]*Blue Ocean Industry, Inc., Gunsan 54002, Republic of Korea*

Bagasse, an abundant form of agricultural waste obtained via sugarcane processing in Southeast Asia, is increasingly used as fuel in biomass plants. However, the ash generated via bagasse combustion, particularly at high alkali contents, can cause significant slagging and fouling in boilers and combustors. In this study, an aluminosilicate-based fuel additive was used to change the properties of ash and mitigate these problems. The ash generated from bagasse combustion exhibited a high potassium oxide content of 18.38 % and a relatively low alumina content, which is expected to result in ash with a low melting temperature. The potassium oxide and calcium oxide contents decreased significantly, whereas the alumina content increased as the additive blend ratio was increased. Four predictive indices, which were calculated from the chemical compositions of the ash, indicated that blending with the additive mitigates ash-related problems compared with those associated with the combustion of bagasse alone. Potassium sulfate was found to be the main mineral phase in the ash of the non-blended sample. Conversely, the additive-blended samples showed higher contents of kalsilite, lomonosovite, and mutinaite, which are minerals with high melting temperatures. Therefore, blending an aluminosilicate-based additive with bagasse can mitigate ash-related problems in boilers and combustors.

Keywords: Fuel additive, Bagasse, Aluminosilicate, Ash fusion.

Introduction

Global interest in the use of renewable fuels, such as waste and biomass, is increasing owing to fossil-fuel depletion, climate change, and environmental problems [1]. The direct combustion of biomass is the most widely used method for producing energy [2]. Biomass has several advantages as a fuel, such as its contents of highly volatile substances and low ash matter, nitrogen, and sulfur [3]. While wood pellets are currently widely used as biofuel, the use of agricultural waste as an alternative is gradually expanding across Asia. Unlike wood pellets, agricultural waste faces challenges due to compositional differences, with slagging and fouling tendencies major issues. The high potassium content in agricultural waste results in the formation of compounds with low melting temperatures; these compounds easily absorb particles and induce severe slagging and fouling in flues or on heating surfaces, leading to reduced efficiency and increased maintenance requirements in biomass plants [4-7]. For instance, biomass power plants often need to be shut down and cleaned for 20–30 d following accumulated slagging and fouling [8]. Currently, most power plants rely on manual cleaning methods that use mechanical tools or vacuum systems to remove slagging and fouling. However, these methods are labor-intensive and inconvenient [9]. Therefore, these problems need to be addressed to enable the effective use of agricultural waste as biofuel.

Slagging refers to the phenomenon in which ash melts and forms deposits on the furnace walls during combustion, while fouling refers to the phenomenon where ash condenses and adheres to a low-temperature section within the heat exchanger of the boiler, where it then hardens along with the combustion gas. Alkali components, such as potassium and sodium, play crucial roles in slagging and fouling by adhering to super- or re-heaters within boilers. Slagging and fouling are also closely related to boiler corrosion. Potassium and sodium react with chlorine to form sodium and potassium chlorides, respectively, during combustion. These products are released with the combustion gases as molten salts at temperatures above 900 °C and generally adhere to the surface of the boiler upon cooling. Chlorides can react with oxide scales to accelerate steel oxidation, resulting in boiler corrosion. These issues, commonly referred to as the "ash chemistry of biomasses," have recently gained considerable research interest, and many studies into the mechanisms of ash formation and ash characteristics have been conducted [10-18].

*Corresponding author:
Tel : +82-43-913-1502
E-mail: leejinh1@kicet.re.kr

Several corrosion-prevention techniques, such as the use of anti-corrosion materials, altering the structure of the boiler, and changing the fuel properties [19-25], have been reported. Anti-corrosion materials, including alumina coatings, resist corrosion within the boiler [21-24]. The boiler contains structural traps that physically remove chlorides and prevent corrosion. Thermochemical conversion methods for removing corrosion-generating materials from fuels have also been reported and include pyrolysis and gasification [26-28]. Although these approaches can significantly reduce corrosion within a boiler, they need to be considered in the initial design of the boiler and use expensive materials, which increases initial investment costs. The use of fuel additives is a simple, viable method that can be used industrially. Blending additives into fuel alters the ash composition generated during combustion, thereby enhancing the melting behavior of the ash by reducing the contents of problematic species [29]. This method can be implemented without changing the material and structure of the boiler or heat exchanger. Currently, sulfate, clay minerals, sulfur-containing char, ammonium sulfate, and ferric sulfate are used as fuel additives [30]. Aluminosilicate-based additives are also used as fuel additives. These materials are highly porous, reactive, and have high melting points and specific surface areas, which are crucial features for their use as additives [31-34]; moreover, they do not affect combustion efficiency or generate pollutants [35, 36]. As they are chemically stable powders, these additives can be easily transported and stored; moreover, they can be used without additional pretreatment [37].

Meanwhile, bagasse, a byproduct of sugarcane, which is abundant in Southeast Asian countries such as Vietnam, India, and Indonesia [38], is a major source of energy in this region, alongside wood residues, rice husks, rice stalks, and oil palm residues [39]. Aluminosilicate-based additives primarily comprise silicon, aluminum, and admixtures of iron and titanium; these elements bind to potassium or sodium within the biomass to suppress the formation of potassium chloride and sodium chloride [40].

This study aimed to address the challenges associated with bagasse, a widely used Southeast Asian biofuel through the use of an aluminosilicate additive. While previous research used high blending ratios that were infeasible for implementation [41, 42], this study examined the aluminosilicate additive using blending ratios that are capable of being used industrially. The effects of blending aluminosilicate-based fuel additives with bagasse on ash characteristics, including the ash composition, phases, and fusion temperature were investigated. Changes in the ash characteristics were used to predict slagging and fouling tendencies during bagasse combustion. Consequently, we explored how to mitigate ash-related issues in boilers and combustors using an aluminosilicate-based additive. This study, therefore, proposes a practical solution to the challenges faced by combustors that use bagasse.

Materials and Methods

Biomass fuel and additive

Bagasse, which was supplied by the Institute for Advanced Engineering (IAE, Yongin, Republic of Korea) was used as the biomass fuel in this study. The IAE imports sugarcane from Vietnam and produces bagasse via juice extraction. The bagasse was used directly without further drying. Bagasse samples were prepared by planetary milling using a Pulverisette 5 mill (Fritsch, Idar-Oberstein, Germany) with 5- and 10-mm-diameter balls used in a 3:7 mass ratio. The sample and balls were loaded at a mass ratio of 1:40. Milling was conducted at a speed of 300 rpm for 5 min. The bagasse was subsequently transferred to a shaking sieve (Analysette 3 PRO, Fritsch) and bagasse particles 200–1000 μm in size were collected.

The aluminosilicate-based material was provided by Blue Ocean Industry, Gunsan, Republic of Korea, and was used as the fuel additive in this study without further treatment.

Ash specimen preparation

Blended bagasse samples were prepared with different additive blend ratios. The additive was first dried overnight at 105 ± 5 °C to constant mass. Blended samples were prepared by placing the fuel additive and bagasse in containers with the desired mass ratios and mixed vigorously using a home mixer (Shinil Industrial, Seoul, Republic of Korea) for 1 min at low speed to produce homogeneous samples. Additive-to-bagasse blend ratios of 0, 3, 5, 7, and 10 wt.% were used. Ash specimens were produced by combusting the blended bagasse samples in a muffle furnace (M-25P, Hantech, Gunpo, Republic of Korea) at 900 °C for 1 h. Combustion was conducted by increasing the temperature at 5 °C/min to 900 °C.

Analytical methods

Proximate analysis, which determines the fixed carbon, moisture, ash, and volatile contents, was conducted according to the American Society for Testing and Materials (ASTM) standards [43, 44]. The carbon, hydrogen, oxygen, and nitrogen contents of the bagasse (ultimate analysis) were measured according to the standard test methods for solid fuel products published by the International Organization for Standardization [45]. The ash composition was analyzed using inductively coupled plasma–optical emission spectrometry (ICP-OES, iCAP 7600 ICP-OES Duo, Thermo Fisher Scientific, Waltham, MA, USA).

Ash samples were mineralogically analyzed by X-ray diffractometry (XRD) using a copper tube (λ = 1.5405 Å, Rigaku, Tokyo, Japan) and relative intensity ratio (RIR)

Table 1. Predictive indices used in this study.

Index	Equation	Criteria	Ref.
Base/acid ratio	$B/A = \frac{Fe_2O_3+CaO+MgO+K_2O+Na_2O}{SiO_2+Al_2O_3+TiO_2}$ (1)	Higher tendency as B/A value approaches unity	[47,48]
Bed agglomeration index	$BAI = \frac{Fe_2O_3}{K_2O+Na_2O}$ (2)	<0.15: High	[49,50]
Fouling index	$FI = R_{\frac{b}{a}} \times (Na_2O + K_2O)$ (3)	<0.6: Low 0.6–40: Medium >40: High	[51]
Slag viscosity index	$SVI = \frac{SiO_2}{SiO_2+Fe_2O_3+CaO+MgO} \times 100$ (4)	>72: Low 63–72: Medium <63: High	[49]

analysis. X-ray radiation was generated at 15 mA and 40 kV, with scattering angles (2θ) in the 10–90° range. The XRD pattern generated via RIR analysis was referenced against data from the International Centre for Diffraction and used to identify the ash compounds synthesized via the co-combustion of bagasse and the additive.

Several slagging and fouling indices were calculated according to the chemical composition of the formed ash to predict fouling and slagging possibilities during combustion. The equations used to determine the base/acid ratio (B/A), as well as the bed agglomeration, fouling, and slag viscosity indices (BAI, FI, and SVI, respectively) are presented in Table 1 as Equations 1–4, respectively (Table 1).

The microstructures of the ash compounds were analyzed by scanning electron microscopy (SEM) using an EM-30 mini-scanning electron microscope (COXEM, Daejeon, Republic of Korea) to investigate their agglomeration tendencies and surfaces.

The ash fusion temperature, as well as the initial deformation, softening, hemispherical, and fluid temperatures (IDT, ST, HT, and FT, respectively) were determined according to ISO 21404-2020 [46]. The shrinkage starting temperature (SST) was determined as the point at which a change in sample volume of approximately 0.5% of the total volume was observed. The blended bagasse samples were pressed into pellets with 0.5-cm heights and diameters using a biomass ash mold (Changsha Kaiyuan Instruments, Changsha, China) to ensure uniformity when examining ash melting behavior. The pellets were placed in an ash fusion determinator (5E-AF4115, Changsha Kaiyuan Instruments) and exposed to oxidizing conditions at a constant heating rate of 5 °C/min.

Data analysis

All tests were performed in triplicate and errors analyzed. The error bars in the various graphs correspond to the standard deviations of the results.

Results and Discussion

Chemical characteristics of the samples

The bagasse used in this study exhibited a high moisture content of 64.0 wt.% and a moderate volatile matter contents of 29.0 wt.% on an as-received basis (Table 2). The gross calorific value of the bagasse is lower than those of general biomasses, which range between 15.41 and 19.52 MJ/kg [52], owing to its high moisture content. Fresh (not dried) bagasse was used as the fuel, with air drying increasing its calorific value, rendering combustion more economically and energetically attractive. Ultimate analysis revealed that the high oxygen content of the bagasse is one of the reasons for its low calorific value. A notable component is nitrogen, at only 0.40 wt.%.

During combustion, the nitrogen within the fuel is converted into gaseous nitrogen or nitric oxide (NOx), which affects the environment significantly. The nitrogen content of the bagasse used in this study is notably lower than those of wood, peanut shells, sunflower stalks, and *Miscanthus* husks, as reported by Rizvi et al [49]. A previous study suggested that solid biofuels

Table 2. Bagasse components.

	Component	Content (wt.%)
Proximate analysis	Fixed carbon	6.3
	Moisture	64.0
	Ash	0.7
	Volatiles	29.0
Ultimate analysis	C	47.22
	H	6.13
	O	44.66
	N	0.40
Gross calorific value (MJ/kg)	7.71	

Table 3. Inorganic compositions of bagasse and the additive.

Content	MgO	Al_2O_3	SiO_2	P_2O_5	SO_3	Cl	K_2O	Na_2O	CaO	TiO_2
Bagasse (wt.%)	11.74	7.93	23.78	6.2	5.23	19.59	18.38	0.27	4.51	0.18
Additive (wt.%)	0.01	14.45	79.04	3.55	0.06	0.02	0.07	0.65	0.04	1.14

may emit NOx at nitrogen contents above 0.6 wt.% [53]. According to its nitrogen content, the bagasse used in this study has a low probability of emitting NOx when used as a fuel.

The bagasse mainly contained silicon dioxide (23.78%), potassium oxide (18.38%), and magnesium oxide (11.74%, Table 3); its relatively low alumina content was expected to lead to low ash melting temperatures [54]. Alumina is a refractory ceramic oxide with a melting temperature of 2004 ℃. In contrast, the additive has a high alumina content (14.45 %); consequently, blending bagasse with the aluminosilicate-based additive is expected to enhance its ash melting characteristics owing to the higher alumina content. Bagasse contains 19.59% chlorine, whereas other biomasses, such as rice husks, wheat straw, and wood pellets, only contain 0.01–0.1% chlorine [55]. Typically, chlorine reacts with potassium during combustion to form potassium chloride, which is the main cause of high-temperature corrosion owing to its low melting temperature [56]. The direct combustion of bagasse in this study resulted in significant high-temperature corrosion owing to its high potassium and chlorine contents.

Chemical compositions of ash samples and predictive indices

The contents of the major inorganic elements in the additive-blended and unblended ash are shown in Fig. 1. The bagasse contains major inorganics, such as potassium oxide, magnesium oxide, and silicon dioxide (Fig. 1). However, the blended samples exhibited different major inorganics in their ash samples (i.e., silicon dioxide and alumina), which are the main components of the additive. The potassium oxide, magnesium oxide, and calcium oxide contents decreased significantly as the blend ratio of the additive was increased, whereas the alumina content increased. The silicon dioxide content in the ash produced from the 0% blended sample (containing only bagasse) exceeded its alumina content. On the other hand, the alumina content exceeded the silicon dioxide content in the ash derived from the sample blended with the fuel additive, owing to the introduction of alumina from the fuel additive into the ash. As alumina has a high melting temperature, a higher alumina content increases the possibility of forming compounds with high melting temperatures.

The contents of the inorganic components shown in Fig. 1 were used to calculate the slagging and fouling indices. The predictive indices of the non-blended and blended samples differ significantly (Fig. 2). In the absence of the additive, the indices were observed to fall outside of the specific ranges of criteria where positive trends may occur; consequently, the use of bagasse alone is more likely to lead to slagging and fouling. The slagging tendency of the ash increases as the B/A value approaches unity, whereas the ash is likely to exhibit a low slagging probability when the B/A value deviates from unity. The ash generated solely from bagasse exhibits a B/A of 1.36 and a high slagging tendency (Fig. 2); however, the B/A was significantly lower (<0.5) after blending with the additive. The 3, 5, 7, and 10 wt.% blended ash samples exhibited B/A values of 0.13, 0.13, 0.10, and 0.09, respectively (Fig. 2(a)); hence, blending bagasse with the additive reduces the slagging tendency. The BAI is used to evaluate operational problems associated with a low ash fusion temperature. A previous study determined that bed agglomeration occurs at BAI values below 0.15 [46]. The bagasse ash in the present study exhibited a BAI of 0.06, which increased to 0.16, 0.36, 0.34, and 0.27 as the additive blend ratio was increased to 3, 5, 7, and 10 wt.%, respectively (Fig. 2(b)). Based on these BAIs, we predict that using the fuel additive employed in this study reduces the agglomeration tendency during combustion. The FI is an indicator of ash deposition tendency; the bagasse ash exhibited an FI of 34.90, whereas FI values of 0.97, 0.53, 0.33, and 0.25 were determined for the 3, 5, 7, and 10 wt.% blended samples, respectively (Fig. 2(c)). Based on these results, we predict that blending bagasse with the additive reduces the fouling tendency. The SVI is an indicator of the slagging tendency, which is high at values below 63. An SVI of less than 63 was obtained without the additive; this value exceeded 72 with the additive, indicative of low slagging tendencies

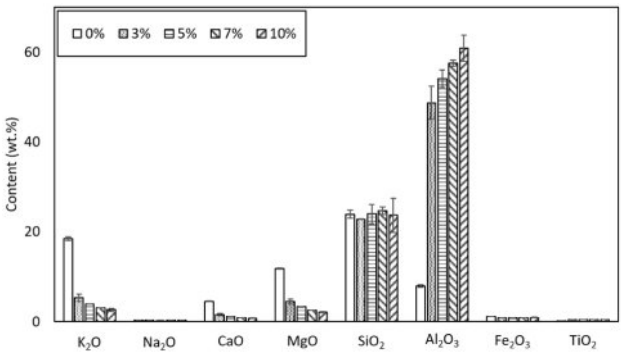

Fig. 1. Main inorganic components of ash from each blended sample.

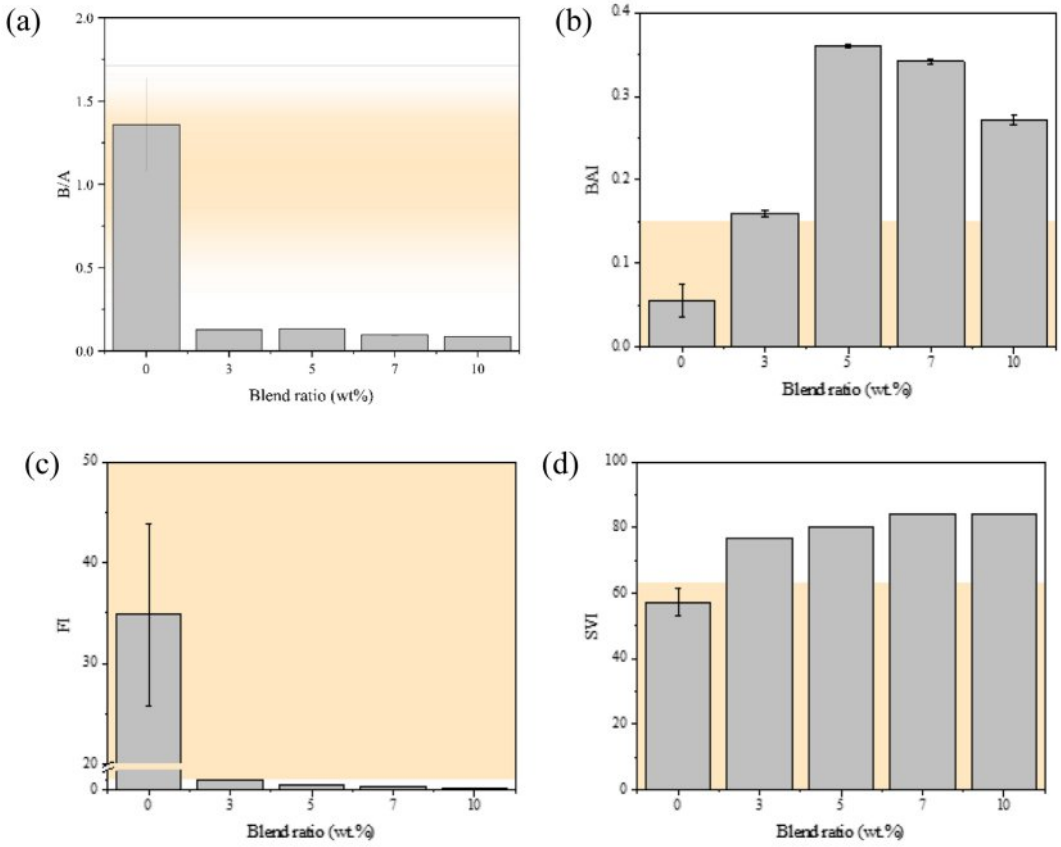

Fig. 2. Predictive indices: (a) base:acid ratio (B/A), (b) bed agglomeration index (BAI), (c) fouling index (FI), and (d) slag viscosity index (SVI) as functions of the additive blend ratio. The yellow regions indicate the ranges where negative tendencies occur.

in all cases (Fig. 2(d)).

Mineralogical analyses of the ash samples

In this study, we employed an aluminosilicate-based additive to reduce the possibility of boiler corrosion in bagasse biomass plants. The aluminosilicate-based additive should capture potassium in the bottom ash to form ash with a higher melting temperature and a more favorable phase composition, which helps to prevent slagging problems. Therefore, whether or not the ash changes to a high-melting-temperature phase was investigated by identifying the mineral phases within the ash by XRD. Fig. 3(a) shows the key peaks of the major mineral phases. The XRD pattern of the non-blended sample (bagasse only) differs significantly from those of the blended samples. The main mineral phase in the non-blended ash is potassium sulfate (61%, Fig. 3), which has a low melting temperature of 680 °C [57]. The peaks related to potassium sulfate are less intense in the patterns of the blended samples, indicative of less potassium sulfate (Fig. 3). Conversely, high-melting-temperature phases, such as trikalsilite, kalsilite, megakalsilite, lomonosovite, and mutinaite, are more abundant (Fig. 3(a)). Mutinaite, kalsilite, and microcline melt at 1200, 1750, and 1150 °C, respectively [58, 59]; hence, the use of a fuel additive can increase the melting temperatures of ash phases. Compounds with low melting temperatures lead to the formation of molten or sticky ash particles that agglomerate, impact, or condense on heat-transfer surfaces, thereby reducing boiler efficiency. Consequently, the formation of high-melting-point phases mitigates the slagging and fouling tendencies, ultimately reducing the possibility of corrosion. The following chemical reactions in which the potassium in bagasse and the fuel additive form high-melting-temperature phases are inferred:

$$Al_2Si_2O_7(s) + 2KCl(g) + 2NaCl(g) \rightarrow 2KNaAlSi_3O_{8(S)}\ (\text{Microcline}) + Cl_2(g) \quad (5)$$

$$Al_2Si_2O_7(s) + 2KCl(g) + H2O(g) \rightarrow 2KAlSiO_{4(S)}\ (\text{Kalsilite}) + Cl_2(g) \quad (6)$$

$$Al_2Si_2O_7(s) + 4KCl(g) \rightarrow 2K_2Al_2Si_3O_{8(S)}\ (\text{Megakalsilite}) + Cl_2(g) \quad (7)$$

$$2Al_2Si_2O_7(s) + 2KCl(g) \rightarrow K_2Al_2Si_4O_{11(S)}\ (\text{Mutinaite}) + Cl_2(g) \quad (8)$$

Changes in ash fusion temperature

Mineralogical analysis revealed the formation of high-melting-temperature phases when the additive was used.

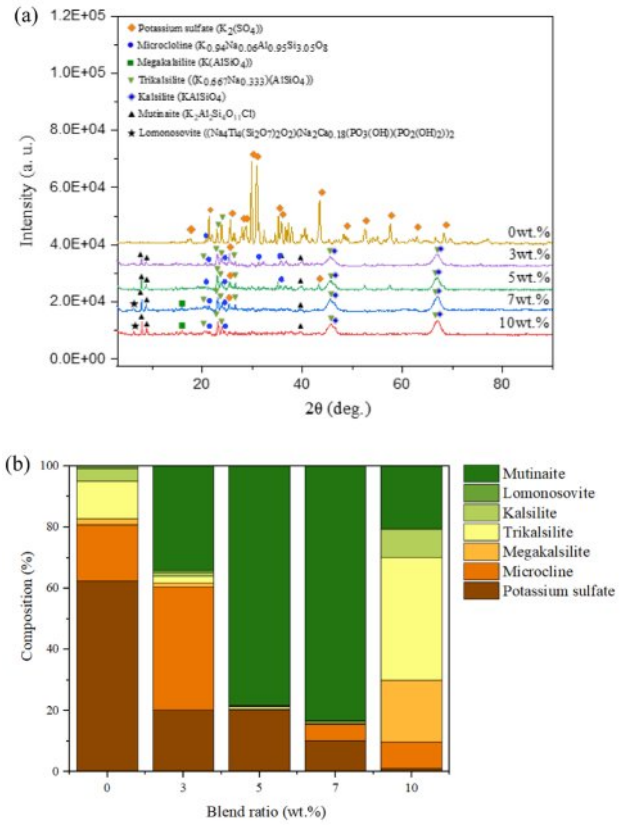

Fig. 3. (a) XRD patterns of bagasse ash with different additive blend ratios, with key peaks corresponding to the major mineral phases highlighted. (b) Relative compositions of the major mineral phases.

Table 4. Ash melting properties of bagasse with and without the additive.

Blend ratio (wt.%)	0	3	5	7	10
SST (°C)	1010	1060	1140	1140	1160
IDT (°C)	1080	1370	1450	>1500	>1500
HT (°C)	1150	1450	>1500	>1500	>1500
FT (°C)	1200	1490	>1500	>1500	>1500

We examined how these phases affect the ash fusion temperature by measuring the SST, IDT, HT, and FT values, the results of which are shown in Table 4. The bagasse ash (unblended) began to melt at 1080 °C and had completely melted at 1200 °C, consistent with a high possibility of melting at relatively low temperatures and ash liquefaction above 1200 °C. The addition of the additive led to higher IDTs, with values of 1370 and 1450 °C recorded for the 3 and 5 wt.% blended samples, which corresponds to improvements of 26.9% and 34.3%, respectively (Table 4). No deformation was observed, even at 1500 °C at blending ratios of 7 wt.% or greater, and the shape of the ash remained intact. Additionally, the use of the additive increased the FT by approximately 300 °C. The ash did not liquefy at 1500 °C when blended at ≥5 wt.%, suggestive of low melting possibilities. These improvements are attributable to the formation of more high-melting-temperature phases, such as kalsilite and mutinaite. The effects of aluminosilicate-based additives, specifically coal pulverized fuel ash and

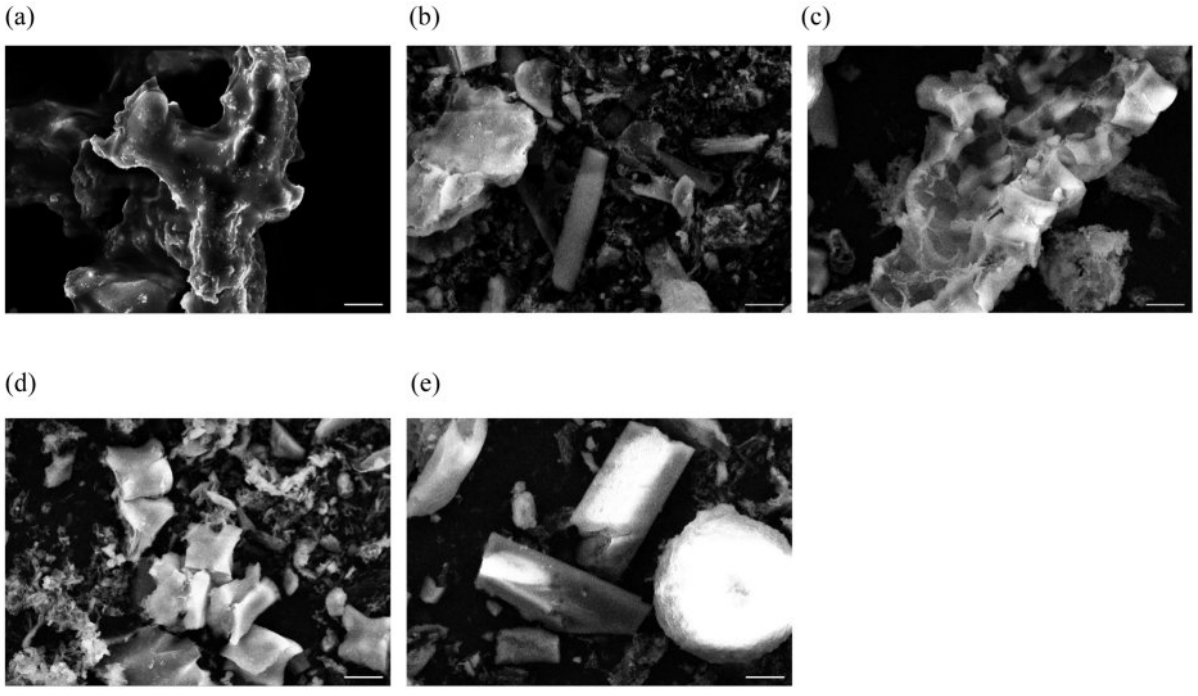

Fig. 4. SEM images of ash generated from (a) bagasse and (b–e) blended bagasse with 3, 5, 7, and 10 wt.%. of the additive. Scalebars: 10 μm.

kaolinite, on the ash melting properties of olive cake and white wood have previously been investigated [60]. The use of 5% pulverized fuel ash and kaolinite led to increases of 9.9% and 21.4%, respectively, in the IDT of olive cake, but did not significantly affect the IDT of white wood. In comparison, the fuel additive used in this study improved the IDT more effectively.

The effect of increasing the ash fusion temperature is clearly observed in the SEM images shown in Fig. 4. The ash generated solely from bagasse exhibited irregular particles that are tens of micrometers in size, along with coalesced aggregates of particles. The sticky phase acts as a glue that binds particles to form agglomerates (Fig. 4(a)). Several of the ash particles melted into large particles, and other particles adhered to them. Less melting was observed on the surface of the ash as the blend ratio was increased; hence the shape of each particle was maintained (Figs. 4(b–e)).

The objective of this study was to address industrial challenges associated with bagasse as a biofuel. Therefore, we examined fuel additive blend ratios that are industrially applicable (3, 5, 7, and 10 wt.%) as opposed to the impractical level of 20 wt.% used in previous studies [41, 42]. This study revealed that the properties of the ash improved consistently with increasing additive blend ratio. The melting properties of the ash were observed to improve even at the lowest blend ratio examined in this study (i.e., 3 wt.%). However, the optimal blend ratio for mitigating combustor corrosion needs to be examined under real field conditions. In this context, mitigating combustor corrosion needs to be considered along with economic factors and overall fuel performance.

Although the blend ratios of the fuel additive used in this study were lower than those used in previous studies, they were still significantly higher than the ash content of bagasse, which suggests that the fuel additive and the ash components in bagasse react ineffectively. Future studies should focus on improving the reactivity between the fuel additive and the ash components in biomass.

Conclusions

The effects of an aluminosilicate additive on the properties of bagasse ash, including the ash composition, phases, and fusion temperature, were investigated at different blend ratios. Bagasse, which is rich in potassium, was expected to exhibit a low ash melting temperature. Significantly lower potassium oxide and calcium oxide contents were observed in the ash following blending with the additive, along with slightly less magnesium oxide. Four predictive indices related to slagging and fouling were calculated to investigate the slagging and fouling tendencies according to the chemical compositions of the ash samples of the blended specimens. These indices revealed high slagging and fouling tendencies when bagasse was used alone, which diminished when bagasse was blended with the aluminosilicate additive. The ash produced using bagasse alone contained the largest proportion of potassium sulfate, which is characterized by its low melting temperature. However, the proportions of phases with higher melting temperatures, such as kalsilite, lomonosovite, and mutinaite, increased as the blend ratio of the additive was increased, which is supported by ash-fusion-temperature analyses. The four ash fusion temperatures—shrinkage start, initial deformation, hemispherical, and fluid—were notably higher when blended with the additive, which was also evident in the SEM images of the ash samples.

These findings highlight the potential of mitigating the effects of slagging and fouling in boilers or combustors that use bagasse as a fuel and the aluminosilicate fuel additive used in this study. This approach is promising for addressing the operational challenges of boilers and combustors across Southeast Asia that rely on bagasse as a fuel. The method of properly mixing and injecting the fuel additive with bagasse fuel significantly influences the additive's performance. Furthermore, employing additive with a fine particle size distribution also plays a crucial role in determining their effectiveness. These factors should be carefully considered in future research.

Acknowledgment

This work was supported by the Korea Agency for Infrastructure Technology Advancement (KAIA) through the overseas demonstration and business model development of a 6 MW class tri-generation plant with unused renewable fuel based on modularization, which was funded by the Ministry of Land, Infrastructure and Transport in Korea [grant number RS-2021-KA161883].

References

1. Y. Wang, Y. Liu, Z. Xu, K. Yin, Y. Zhou, J. Zhang, P. Cui, S. Ma, Y. Wang, and Z. Zhu, Renew. Sust. Energy Rev. 189 (2024) 114015.
2. D. Glushkov, G. Nyashina, R. Anand, and P. Strizhak, Process Saf. Environ. Prot. 156 (2021) 43-56.
3. Y. Zhu, Y. Niu, H. Tan, and X. Wang, Front. Energy Res. 2 (2014) 7.
4. X. Wei, U. Schnell, and K.R. Hein, Fuel 84[7-8] (2005) 841-848.
5. M. Broström, H. Kassman, A. Helgesson, M. Berg, C. Andersson, R. Backman, and A. Nordin, Fuel Process. Technol. 88[11-12] (2007) 1171-1177.
6. A.-L. Elled, K. Davidsson, and L.-E. Åmand, Biomass Bioenergy 34[11] (2010) 1546-1554.
7. A. Mlonka-Mędrala, A. Magdziarz, I. Kalemba-Rec, and W. Nowak, Energy Convers. Manage. 187 (2019) 15-28.
8. Y. Niu, H. Tan, X. Wang, Z. Liu, Y. Liu, and T. Xu, Energy Fuels 24[3] (2010) 2127-2132.
9. Biomass Magazine, Efficient cleaning of sustainable biomass boilers (2022).
10. F. Li, B. Yu, W. Zhao, J. Wang, M. Xu, H. Fan, J. Huang, and Y. Fang, Fuel 323 (2022) 124446.
11. F. Li, C. Zhao, H. Fan, M. Xu, Q. Guo, Y. Li, L. Wu, T. Wang, and Y. Fang, Energy 251 (2022) 123912.

12. Z. Yang, F. Li, M. Ma, H. Fan, X. Liu, and Y. Fang, J. Environ. Chem. Eng. 12[3] (2024) 112863.
13. Y. Wang, L. Jia, B. Guo, B. Wang, L. Zhang, X. Zheng, J. Xiang, and Y. Jin, Waste Manage. 145 (2022) 83-91.
14. Z. Yang, F. Li, M. Ma, W. Zhao, X. Liu, Y. Wang, Z. Li, and Y. Fang, Waste Manage. 174 (2024) 328-339.
15. H. Wang, T. Zhou, X. Tan, N. Hu, Y. Wang, H. Yang, and M. Zhang, Fuel 356 (2024) 129586.
16. Y. Liu, W. Tan, S. Liang, and X. Pan, Fuel 358 (2024) 130068.
17. H. Mörtenkötter, M. Kulkarni, L. Fuchs, F. Kerscher, S. Fendt, and H. Spliethoff, Fuel 374 (2024) 132471.
18. J.H. Park, D.-H. Lee, K.-H. Han, J.-S. Shin, D.-H. Bae, T.-E. Shim, J.H. Lee, and D. Shun, Fuel 236 (2019) 792-802.
19. J. Zhang, H. Gao, D. Lian, N. Luo, J. Wu, and C. Wang, J. Ceram. Process. Res. 26[2] (2025) 209-218.
20. S. Shanmugam, S. Mahalingam, and A. Ranjithkumar, J. Ceram. Process. Res. 24[3] (2023) 495-502.
21. J. Pettersson, C. Pettersson, N. Folkeson, L.G. Johansson, E. Skog, and J.E. Svensson, Materials Science Forum 522-523 (2006) 563-370.
22. Y. Kawahara, Corros. Sci. 44[2] (2002) 223-245.
23. P. Henderson, P. Szakalos, R. Pettersson, C. Andersson, and J. Högberg, Mater. Corros. 57[2] (2006) 128-134.
24. K. Khantisopon, S. Singh, J. Jitputti, C.C. Berndt, and A.S. Ang, High Temp. Corros. Mater. 101 (2024) 1-55.
25. J.R. Keiser, W. Sharp, and D.L. Singbeil, Tappi J. 13[8] (2014) 51-63.
26. Z. Ahmad, in "Principles of corrosion engineering and corrosion control" (Elsevier, 2006)
27. S. Zhang, Y. Su, K. Ding, and H. Zhang, Energy 186 (2019) 115888.
28. S.B. Saleh, B.B. Hansen, P.A. Jensen, and K. Dam-Johansen, Energy Fuels 27[12] (2013) 7541-7548.
29. L. Wang, J.E. Hustad, Ø. Skreiberg, G. Skjevrak, and M. Grønli, Energy Procedia 20 (2012) 20-29.
30. Í.W. França, S.J. Cartaxo, M. Bastos-Neto, L.R. Gonçalves, and F.A. Fernandes, Emiss. Control Sci. Technol. 6 (2020) 105-112.
31. G. Mahmoudzadeha, S.A. Khorramia, S.S. Madania, and M. Frounchib, J. Ceram. Process. Res. 13[4] (2012) 368-372.
32. H. Murray, Clay Miner. 34[1] (1999) 39-49.
33. F. Bergaya and G. Lagaly, Dev. Clay Sci. 1 (2006) 1-18.
34. M.G. Xavier and S.F. Banda, Orient. J. Chem. 32 (2016) 2401-2406.
35. C. Chen, Y. Huang, S. Qin, D. Huang, X. Bu, and H. Huang, Energy 194 (2020) 116889.
36. T. Zeng, A. Pollex, N. Weller, V. Lenz, and M. Nelles, Fuel 212 (2018) 108-116.
37. Y. Fan, Q. Lyu, Z. Zhu, and H. Zhang, J. Energy Inst. 93[4] (2020) 1651-1665.
38. A. Anukam, S. Mamphweli, P. Reddy, E. Meyer, and O. Okoh, Renew. Sust. Energy Rev. 66 (2016) 775-801.
39. M.M. Tun, D. Juchelková, M.M. Win, A.M. Thu, and T. Puchor, Resour. 8[2] (2019) 81.
40. K. Mroczek, S. Kalisz, M. Pronobis, and J. Sołtys, Fuel Process. Technol. 92[5] (2011) 845-855.
41. F. Li, X. Wang, C. Zhao, Y. Li, M. Guo, H. Fan, Q. Guo, and Y. Fang, Bioresour. Technol. 299 (2020) 122515.
42. W. Yang, D. Pudasainee, R. Gupta, W. Li, Z. Song, B. Wang, and L. Sun, Energy Fuels 34[12] (2020) 15399-15410.
43. ASTM D3172-13, Standard practice for proximate analysis of coal and coke (2021).
44. ASTM D7582-15, Standard test methods for proximate analysis of coal and coke by macro thermogravimetric analysis (2023).
45. ISO16993:2015, Solid biofuels – Conversion of analytical results from one basis to another (2015).
46. ISO 21404:2020, Solid biofuels – Determination of ash melting behavior (2020).
47. R. García, C. Pizarro, A. Álvarez, A.G. Lavín, and J.L. Bueno, Fuel 148 (2015) 152-159.
48. M. Reinmöller, M. Klinger, M. Schreiner, and H. Gutte, Fuel 151 (2015) 118-123.
49. T. Rizvi, P. Xing, M. Pourkashanian, L. Darvell, J. Jones, and W. Nimmo, Fuel 141 (2015) 275-284.
50. T. Bridgeman, L. Darvell, J. Jones, P. Williams, R. Fahmi, A. Bridgwater, T. Barraclough, I. Shield, N. Yates, and S. Thain, Fuel 86[1-2] (2007) 60-72.
51. A. Garcia-Maraver, J. Mata-Sanchez, M. Carpio, and J.A. Perez-Jimenez, J. Energy Inst. 90[2] (2017) 214-228.
52. M. Erol, H. Haykiri-Acma, and S. Küçükbayrak, Renew. Energy 35[1] (2010) 170-173.
53. E. Virmond, R.L. Schacker, W. Albrecht, C.A. Althoff, M. de Souza, R.F. Moreira, and H.J. José, Energy 36[6] (2011) 3897-3906.
54. R. Shao, X. Liu, H. Li, and H. Zhou, Ceram. Int. 49[22] (2023) 34603-34615.
55. D.S. Clery, P.E. Mason, C.M. Rayner, and J.M. Jones, Fuel 214 (2018) 647-655.
56. P. Lu, Q. Huang, A.T. Bourtsalas, N.J. Themelis, Y. Chi, and J. Yan, J. Environ. Sci. 78 (2019) 13-28.
57. X. Li, F. He, F. Behrendt, Z. Gao, J. Shi, and C. Li, Fuel 289 (2021) 119754.
58. H. Tan, J. Ceram. Process. Res. 13[6] (2012) 767-769.
59. N. Brachhold and C.G. Aneziris, Int. J. Appl. Ceram. Technol. 10[4] (2013) 707-715.
60. L.J. Roberts, P.E. Mason, J.M. Jones, W.F. Gale, A. Williams, A. Hunt, and J. Ashman, Biomass Bioenergy 127 (2019) 105284.